



Assessing urbanization's contribution to warming in mainland China using satellite-estimated air temperature data

Progress in Physical Geography

1–19

© The Author(s) 2021

Article reuse guidelines:

sagepub.com/journals-permissions

DOI: 10.1177/0309133321988850

journals.sagepub.com/home/ppg

Rui Yao

Key Laboratory of Regional Ecology and Environmental Change, School of Geography and Information Engineering, China University of Geosciences, China

Lunche Wang

Key Laboratory of Regional Ecology and Environmental Change, School of Geography and Information Engineering, China University of Geosciences, China

Xin Huang

School of Remote Sensing and Information Engineering, Wuhan University, China; State Key Laboratory of Information Engineering in Surveying, Mapping and Remote Sensing, Wuhan University, China

Xiaojun Wu

Key Laboratory of Regional Ecology and Environmental Change, School of Geography and Information Engineering, China University of Geosciences, China

Liu Yang

Key Laboratory of Regional Ecology and Environmental Change, School of Geography and Information Engineering, China University of Geosciences, China

Zigeng Niu

Key Laboratory of Regional Ecology and Environmental Change, School of Geography and Information Engineering, China University of Geosciences, China

Abstract

The global surface air temperature (T_a) has increased significantly in the past several decades. However, it remains disputable how much effect rapid urbanization has had on warming trends in mainland China. In this study, a gridded T_a dataset was created using satellite data. Then, a series of satellite-based methods to evaluate the contribution of urbanization to warming were developed. Subsequently, the contribution of urbanization to warming during 2001–2018 was estimated. The national average T_a was found to have increased significantly ($0.23^\circ\text{C}/\text{decade}$) in mainland China. At the national scale, the contribution of urbanization to warming was negligible (less than 1%) since built-up areas account for only approximately 2.66% of

Corresponding author:

Lunche Wang, Key Laboratory of Regional Ecology and Environmental Change, School of Geography and Information Engineering, China University of Geosciences, Wuhan 430074, China.

Email: wang@cug.edu.cn

the area of China. At the regional scale, the contribution of urbanization was also small in most areas and was even negative in some areas. At the local scale, the contributions of urbanization to warming were 53.18%, 54.30% and 47.25% for the mean, maximum and minimum T_a , respectively, averaged for 31 major cities. This study demonstrated that the contribution of urbanization to warming was significant at the local scale, while the contribution of urbanization to large-scale warming was limited. The contribution of urbanization was underestimated at the local scale but overestimated at the national and regional scales by many previous studies due to the sparse and uneven distribution of meteorological stations.

Keywords

Air temperature, urban heat island, remote sensing, urbanization, regional warming, mainland China

1 Introduction

Global surface air temperature (T_a) has increased significantly in the past several decades, causing several severe issues, such as glacier retreat (Roe et al., 2016), permafrost degradation (Shakhova et al., 2017), perturbations in ecosystems (Prävālie, 2018) and increased frequency of heat waves (Luo and Lau, 2017; Sun et al., 2014). Thus, it is vitally important to accurately reveal the magnitude and associated drivers of global warming.

One of the drivers of warming is urbanization, which can cause the urban heat island (UHI) effect that contributes to warming (Ren and Zhou, 2014). The contribution of urbanization to warming at the global scale is small (Hansen et al., 2010; Parker, 2006; Zhao and Wu, 2017). However, it remains in dispute how much rapid urbanization has contributed to warming in mainland China at the national scale (Jin et al., 2018; Li et al., 2019; Ren and Ren, 2011; Ren and Zhou, 2014; Shi et al., 2019; Sun et al., 2016; Wang et al., 2015a). For example, Ren and Zhou (2014) found that the contribution of urbanization to the increase in mean T_a in mainland China was 15.4% over the period 1961–2008. Wang et al. (2015a) found a negligible contribution (approximately 0.35%) of urbanization to the warming trend in mainland China for the period 1951–2010. Sun et al. (2016) found that the contribution of urbanization to warming was approximately one-third in

mainland China during 1961–2013. These studies used data from meteorological stations (the numbers of stations for these studies were different) to analyze the contribution of urbanization to warming. Their study areas and definitions of the contribution of urbanization were the same, and the study periods were generally similar, but the results were quite different. As a result, the contribution of urbanization to warming in mainland China needs to be further investigated. At the local scale, we recognize that the contribution of urbanization to warming was great (generally between 10 and 40%) (Liao et al., 2017; Wang and Ge, 2012; Wang et al., 2015b; Yang et al., 2011; Zhao et al., 2014).

Most of the previous studies used meteorological stations to examine the effect of urbanization on warming trends (Jin et al., 2018; Liao et al., 2017; Park et al., 2017; Ren and Zhou, 2014; Sun et al., 2016; Wang et al., 2015a). The commonly used method is to compare the trends of T_a between urban and rural meteorological stations (Karl et al., 1988; Liao et al., 2017; Mohsin and Gough, 2010; Park et al., 2017; Wang et al., 2015b). However, this method may lead to uncertainties: (1) most of the meteorological stations are situated in or around built-up urban areas (Sun et al., 2016; Wang et al., 2015a). It is difficult to select purely rural stations that are surrounded by land cover types other than built-up urban areas. For instance, Wang et al. (2015a) defined rural stations as

those stations having a proportion of urban area less than 10% within a radius of 11 km. Therefore, the rural stations used in previous studies may undergo urbanization, which causes an underestimation of the urbanization effect. (2) Urbanizing areas generally showed higher increasing trends of UHIs than stable urban areas (SUAs) (Yao et al., 2017; Zhao and Wu, 2017). However, due to the sparse distribution of meteorological stations, previous studies often used one station to represent the Ta of an entire city (Liao et al., 2017; Wang et al., 2015a; Yang et al., 2011). The contribution of urbanization may be overestimated when the station is located in urbanizing areas. Similarly, the contribution of urbanization may be underestimated when the station is located in SUAs or exurban areas. (3) The number of meteorological stations is sparse in western China (Niu et al., 2018; Ren and Zhou, 2014; Sun et al., 2016). For instance, Wang et al. (2015b) showed that there were no meteorological stations in certain $2.5^\circ \times 2.5^\circ$ latitude–longitude grid boxes in western China. Another widely used method is to compare the trends of Ta between meteorological stations and reanalysis data, since the reanalysis data are insensitive to land use changes (Fall et al., 2010; Kalnay and Cai, 2003; Kalnay et al., 2006; Park et al., 2017; Wang and Yan, 2015; Zhou et al., 2004). However, the quality of reanalysis data was relatively low, and the trends of Ta differed substantially for different reanalysis data (Wang and Yan, 2015; Xu et al., 2018). Overall, a new method to quantify the contribution of urbanization to warming, and to avoid the aforementioned uncertainties, needs to be introduced.

Satellite sensors can provide spatially continuous monitoring of the land surface, which can avoid the aforementioned uncertainties. Satellite-based land surface temperature (Ts) and Ta are often strongly related, although the relationship has spatiotemporal variations and depends on land cover type and vegetation (Good et al., 2017; Shiflett et al., 2017; Weng, 2009; Xu

et al., 2018). The relationship between Ts and Ta can be built and then the areas without Ta observations can be predicted using this relationship and spatially continuous Ts data. Thus, spatially continuous Ta data can be mapped. This method has been widely used to estimate Ta from local to global scales (Benali et al., 2012; Hooker et al., 2018; Li et al., 2018; Xu et al., 2018; Zhu et al., 2013). In the present study, the seasonal average Ta was first mapped using Moderate Resolution Imaging Spectroradiometer (MODIS) Ts data. Next, since the station-based point data are different from satellite-based gridded data, a series of satellite-based methods to evaluate the contribution of urbanization to warming was developed. Finally, the contribution of urbanization to warming was systematically examined at the national, regional and local scales in mainland China for the period of 2001–2018.

II Study area and data

I Study area

Mainland China covers approximately 9.6 million km^2 (Figure 1). In mainland China, temperature and precipitation decrease gradually from south to north and from southeast to northwest, respectively. Moreover, recent decades have observed rapid economic development and urbanization in mainland China: (1) the urban population increased from 310.02 million in 1990 to 775.35 million in 2015 (United Nations, 2018), and (2) the real gross domestic product (GDP) increased from 1.87 trillion yuan in 1990 to 68.91 trillion yuan in 2015.

2 Data

Land cover information in 2000, 2005, 2010 and 2015 was derived from the China's Land Use/Cover Datasets (CLUDs). CLUDs have national coverage, high spatial resolution (30 m) and high accuracy (greater than 90%) (Kuang et al., 2016; Liu et al., 2014). Daily mean, maximum and minimum Ta data from 699

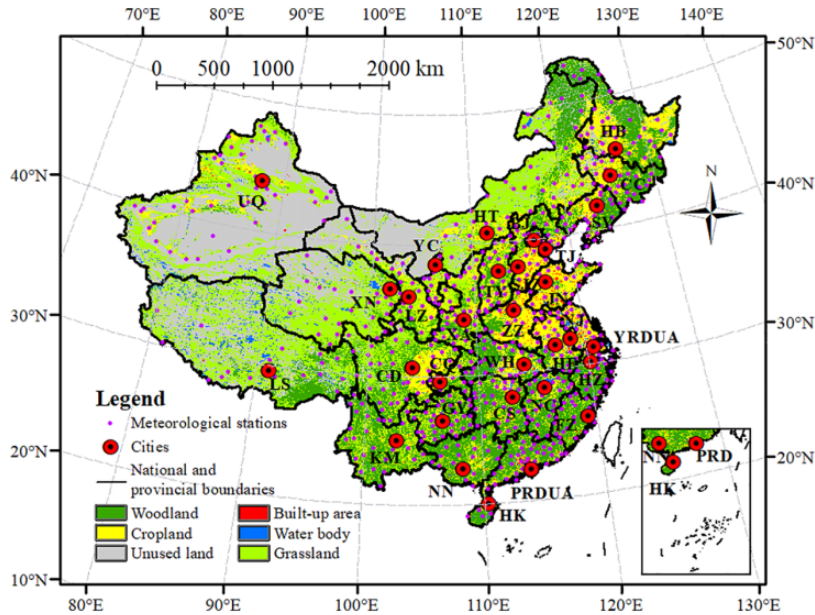


Figure 1. Locations of meteorological stations and 31 cities (or urban agglomerations) in mainland China. BJ: Beijing; HT: Hohhot; SJZ: Shijiazhuang; TY: Taiyuan; TJ: Tianjin; CC: Changchun; HB: Harbin; SY: Shenyang; LZ: Lanzhou; UQ: Urumqi; XA: Xi'an; XN: Xining; YC: Yinchuan; FZ: Fuzhou; HZ: Hangzhou; HF: Hefei; JN: Jinan; NC: Nanchang; NJ: Nanjing; YRDUA: Yangtze River Delta urban agglomeration; CS: Changsha; HK: Haikou; NN: Nanning; WH: Wuhan; ZZ: Zhengzhou; PRDUA: Pearl River Delta urban agglomeration; CD: Chengdu; CQ: Chongqing; GY: Guiyang; KM: Kunming; LS: Lhasa. The background map is the 2015 China Land Use/Cover Dataset.

meteorological stations for the period of 2001–2018 were derived from the China Meteorological Data Service Center (CMDC). Strict quality control was performed by CMDC, and the data error was nearly zero (Li et al., 2019; Wang et al., 2015b). Data from 694 meteorological stations with missing values less than seven days in a month were used in this study (Figure 1). Additionally, T_s and vegetation information over the period of 2001–2018 was obtained from MODIS 1-km-resolution MOD11A2 T_s and MOD13A3 enhanced vegetation index (EVI) data, respectively (Huete et al., 2002; Yao et al., 2019). Finally, 30-m-resolution Advanced Spaceborne Thermal Emission and Reflection Radiometer (ASTER) Digital Elevation Model (DEM) data were used. These satellite data have been thoroughly validated and

showed good accuracy (Huete et al., 2002; Tachikawa et al., 2011).

III Methods

I Preprocessing

Each of the four (2000, 2005, 2010 and 2015) land cover maps were first merged into two major types: built-up area (urban area, industrial land and rural settlement) and other types (all other land cover types). The four maps were then converted into two types of land cover maps with 1000 m resolution: (1) proportional land cover maps (used to study the effect of urbanization on T_a at the national and regional scales, see sections III.3 and III.4), where for each 1000-m-resolution pixel, the value was set as the proportion of land cover type (built-up

area or other type) within the pixel (using the original 30-m-resolution data); and (2) major land cover type maps (used to study the urbanization effect on T_a at the local scales, see section III.5), where for each 1000 m of pixel resolution, the land cover type was given as the land cover type with the highest proportion within the pixel. That is, if the proportion of built-up areas was higher than 50% (Mertes et al., 2015; Yao et al., 2018; Zhou et al., 2014, 2015), the land cover type of the pixel was set as the built-up area; otherwise, the land cover type was set as the other type. Overall, four proportional land cover maps and four major land cover type maps were generated.

The daily mean, maximum and minimum T_a values were first averaged into the seasonal mean, maximum and minimum T_a (spring: March to May; summer: June to August; autumn: September to November; winter: December to February (Ren and Zhou, 2014; Wang et al., 2015a)). T_s and EVI data were also averaged into seasons. In addition, 30-m-resolution DEM data were aggregated to 1000 m resolution. DEM data were assumed to be constant during 2001–2018.

2 T_a estimation and validation

In this study, the seasonal mean, maximum and minimum T_a were mapped using the following steps:

- (1) T_s , EVI and DEM data were used to estimate T_a . These data were used because, first, these variables significantly correlate with T_a and play important roles in estimating T_a (Chen et al., 2016; Li and Zha, 2019; Lin et al., 2016; Shi et al., 2016; Xu et al., 2018; Yoo et al., 2018; Zhu et al., 2019); and second, these data are publicly available. The values of the pixels where the meteorological stations are located were extracted from the T_s , EVI and DEM data.
- (2) The extracted T_s , EVI and DEM data and the observed T_a from the meteorological stations were input into the model. Cubist model (Quinlan, 1992) in R statistical software ('Cubist' add-on package) was utilized in this study since it has high accuracy. For example, Xu et al. (2018) used 10 machine learning algorithms to estimate T_a , and the results showed that the Cubist model has the highest accuracy. Noi et al. (2017) showed that a Cubist model has a higher accuracy than a multiple linear regression model. T_s , EVI and DEM data served as independent variables and the observed T_a served as the dependent variable. The model can automatically fit a relationship between independent and dependent variables.
- (3) The spatially continuous T_a data in mainland China can be created according to the fitted relationship and spatially continuous T_s , EVI and DEM data.

The accuracy of T_a estimation was evaluated by a 10-fold cross-validation method using the data from 694 stations. The root-mean-square error (RMSE), mean absolute error (MAE) and coefficient of determination (R^2) were calculated to describe the model performance.

3 The contribution of urbanization at the national scale

Trends in the mean, maximum and minimum T_a in mainland China during 2001–2018 were examined using linear regression. The effect of urbanization on the trend of T_a refers to the difference between the trend of T_a with and without urbanization, which is calculated as (Park et al., 2017; Ren and Zhou, 2014; Wang et al., 2015a):

$$UE_1 = T_1 - T_2 \quad (1)$$

where T_1 is the trend of the national average T_a (spatial average for all pixels), and T_2 is the

trend of the national average T_a without the effect of urbanization. Consequently, UE_1 is the effect of urbanization on the trend of T_a at the national scale. T_2 was calculated as follows. In the T_a maps, if the proportion of built-up areas of a pixel is higher than 0% (defined as urbanized pixels), the T_a of this pixel was replaced with the average T_a of those pixels with proportions of built-up areas equal to 0% (defined as nonurbanized pixels) within a radius of 50 km. Subsequently, T_2 is the trend of national average T_a after processing using the abovementioned step. Since all urbanized pixels were replaced using surrounding nonurbanized pixels in the step mentioned above, the pixel numbers for calculating T_1 and T_2 were the same. Additionally, the T_a of nonurbanized pixels for calculating T_1 and T_2 were the same, whereas the T_a of urbanized pixels for calculating T_1 and T_2 were different. Therefore, the urbanization effect can be evaluated accurately. Equation (1) is based on the hypothesis that the trends in T_a of urbanized pixels are the same as the trends in T_a of the surrounding nonurbanized pixels if urbanization does not occur. This hypothesis is the same as using the difference in trends in T_a between urban and rural meteorological stations to represent the urbanization effect in previous studies (Ren and Zhou, 2014; Sun et al., 2016; Wang et al., 2015a).

The contribution of urbanization is defined as the proportion of the effect of urbanization on the trend of T_a to the overall trend of T_a . The contribution of urbanization to warming at the national scale was calculated using equation (2):

$$C_1 = \frac{UE_1}{T_1} \times 100\% \quad (2)$$

where T_1 is the trend of the national average T_a . UE_1 is the effect of urbanization on the trend of T_a . C_1 is the contribution of urbanization at the national scale. Note that the contribution of urbanization was calculated only when T_1 increased (linear regression slope > 0) significantly ($p < 0.1$).

4 The contribution of urbanization at the regional scale

In previous studies, mainland China was divided into a series of $2.5^\circ \times 2.5^\circ$ or $5^\circ \times 5^\circ$ grids, and the effect of urbanization on the observed warming trends was calculated in each grid (Ren and Zhou, 2014; Wang et al., 2015b). Previous studies failed to divide mainland China into smaller grids since the number of meteorological stations is insufficient in western China. Similar to previous studies, all of China was divided into a series of 250×250 km grids, and the contribution of urbanization to warming at the regional scale was calculated in each grid. In addition, the wall-to-wall coverage of satellite data can provide detailed spatial information. In this study, the contribution of urbanization was further mapped using a moving window method. First, an empty image with a size equal to the gridded T_a data was generated. Second, for a pixel in the empty image, a round window that centered this pixel was generated. Third, the value of this pixel was set as the effect of urbanization (or contribution of urbanization) within this window. Fourth, this window moved to the next pixel, and the value of the next pixel was set. This step was repeated until the values of all pixels were set. In this study, three round windows with 50 km radius, 100 km radius and 150 km radius were used. The T_a maps with and without the effects of urbanization (see the previous section) and equation (2) were used to calculate the contribution of urbanization.

5 Urbanization's contribution at the local scale

In the present study, the contribution of urbanization at the local scale was analyzed in 31 major cities or urban agglomerations in mainland China (Figure 1). For each city, four areas were generated using major and proportion land cover maps: (1) whole urban area (WUA), defined as the united areas of built-up areas of the four (in

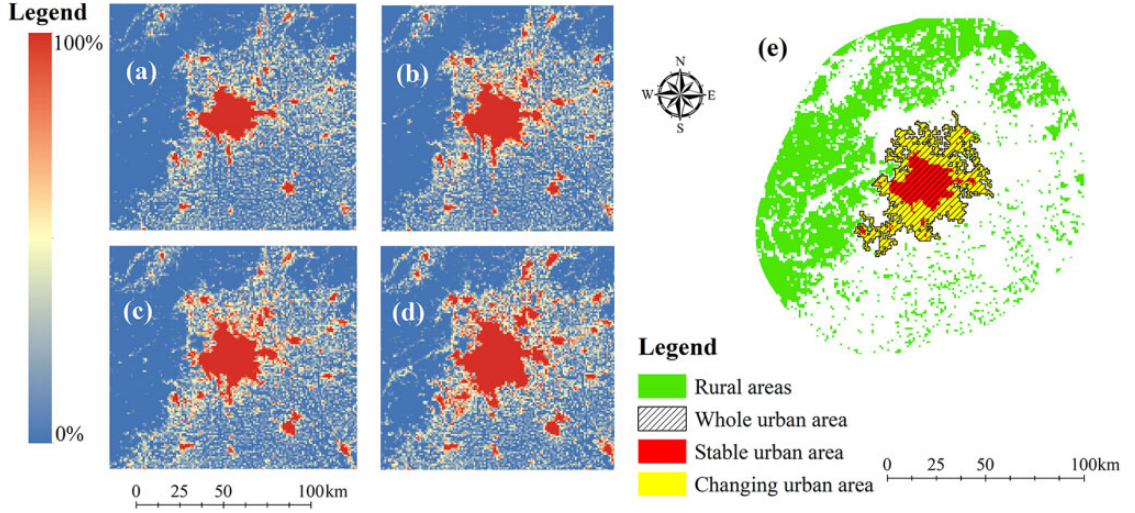


Figure 2. Map of the proportions of built-up areas in (a) 2000, (b) 2005, (c) 2010 and (d) 2015. (e) Schematic diagram of rural area, whole urban areas, stable urban areas and changing urban areas. Beijing was used as an example.

the years 2000, 2005, 2010, 2015) major land cover type maps; (2) SUA, defined as those pixels with proportions of built-up areas that did not change from 2000 to 2015 in the WUA; (3) changing urban area (CUA), referring to those pixels with proportions of built-up areas that changed at least once from 2000 to 2015 in the WUA – in other words, the WUA was divided into two parts, SUA and CUA; and (4) reference rural area, defined as the 50 km buffer around the WUA (removing urbanized pixels) (Imhoff et al., 2010). This distance (50 km) is closer than the distance between urban and reference rural meteorological stations in previous studies (generally between 50 and 150 km) (Fang et al., 2014; Wang et al., 2015a; Yang et al., 2011). A schematic diagram of these four areas is shown in Figure 2. Finally, the effect of urbanization on the trend of T_a at the local scale was calculated using equation (3):

$$UE_2 = T_3 - T_4 \quad (3)$$

where T_3 is the trend of T_a in WUA or SUA or CUA, and T_4 is the trend of T_a in reference rural areas. Thus, UE_2 is the urbanization effects on

trends of T_a at the local scale. The urbanization's contribution was calculated using equation (4):

$$C_2 = \frac{UE_2}{T_3} \times 100\% \quad (2)$$

where T_3 is the trend of T_a in WUA or SUA or CUA. UE_2 is the effects of urbanization on the trend of T_a at the local scale. C_2 is the contribution of urbanization to the trend of T_a at the local scale.

IV Results

1 Validation of the estimated T_a

The Cubist model produced satisfactory T_a estimation accuracy. The MAEs were 0.79, 1.05 and 0.94°C for the mean, maximum and minimum T_a , respectively. The RMSEs were 1.15, 1.51 and 1.31°C for the mean, maximum and minimum T_a , respectively. The R^2 values were 0.99, 0.98 and 0.99 for the mean, maximum and minimum T_a , respectively. The accuracy in this study is higher than the accuracy in the majority of previous studies (RMSE generally between 1 and 3°C) (Benali et al., 2012; Li and Zha, 2019;

Table 1. Trends of Ta, urbanization effects and contributions of urbanization for the period of 2001–2018. The urbanization's contribution was only calculated when the national average Ta increased significantly.

	Slope (°C/decade)	Slope without urbanization (°C/decade)	Urbanization effects (°C/decade)	Urbanization's contribution
Annual mean Ta	0.23*	0.23*	0.00	0.98%
Annual maximum Ta	0.15	0.15	0.00	
Annual minimum Ta	0.30***	0.30***	0.00	0.06%
Spring mean Ta	0.39	0.39	0.01	
Spring maximum Ta	0.36	0.35	0.01	
Spring minimum Ta	0.32*	0.31	0.00	1.06%
Summer mean Ta	0.28	0.28	0.00	
Summer maximum Ta	0.33*	0.33*	0.00	0.70%
Summer minimum Ta	0.40*	0.40*	0.00	0.63%
Autumn mean Ta	0.11	0.11	0.00	
Autumn maximum Ta	−0.20	−0.20	0.00	
Autumn minimum Ta	0.32	0.32	0.00	
Winter mean Ta	0.14	0.14	−0.00	
Winter maximum Ta	0.07	0.07	0.00	
Winter minimum Ta	0.18	0.19	−0.01	

Significance levels: * $p < 0.1$; ** $p < 0.05$; *** $p < 0.01$.

Li et al., 2018; Lu et al., 2018; Noi et al., 2017; Zhang et al., 2016). For example, Li and Zha (2019) estimated the mean Ta in China for the period of 2001–2015. The RMSEs of Li and Zha (2019) ranged from 1.57 to 1.99°C, primarily because this study estimated the seasonal Ta, while most of the previous studies estimated monthly or daily Ta.

2 Temporal trends of Ta in mainland China

The rate of increase of the annual minimum Ta (0.30°C/decade, $p < 0.01$) was higher than for the

maximum (0.15°C/decade, $p = 0.36$) and mean (0.23°C/decade, $p < 0.1$) Ta in mainland China for the period of 2001–2018 (Table 1). The proportion of significant increasing trends of the minimum Ta (39.46%) was higher than the mean (26.14%) and maximum (12.54%) Ta (Figure 3) because the variations in minimum Ta are more affected by the greenhouse effect, while the mean and maximum Ta values are also affected by many other factors, such as solar radiation and atmospheric moisture (Ren et al., 2017; Wang et al., 2018). Seasonally, higher increasing rates

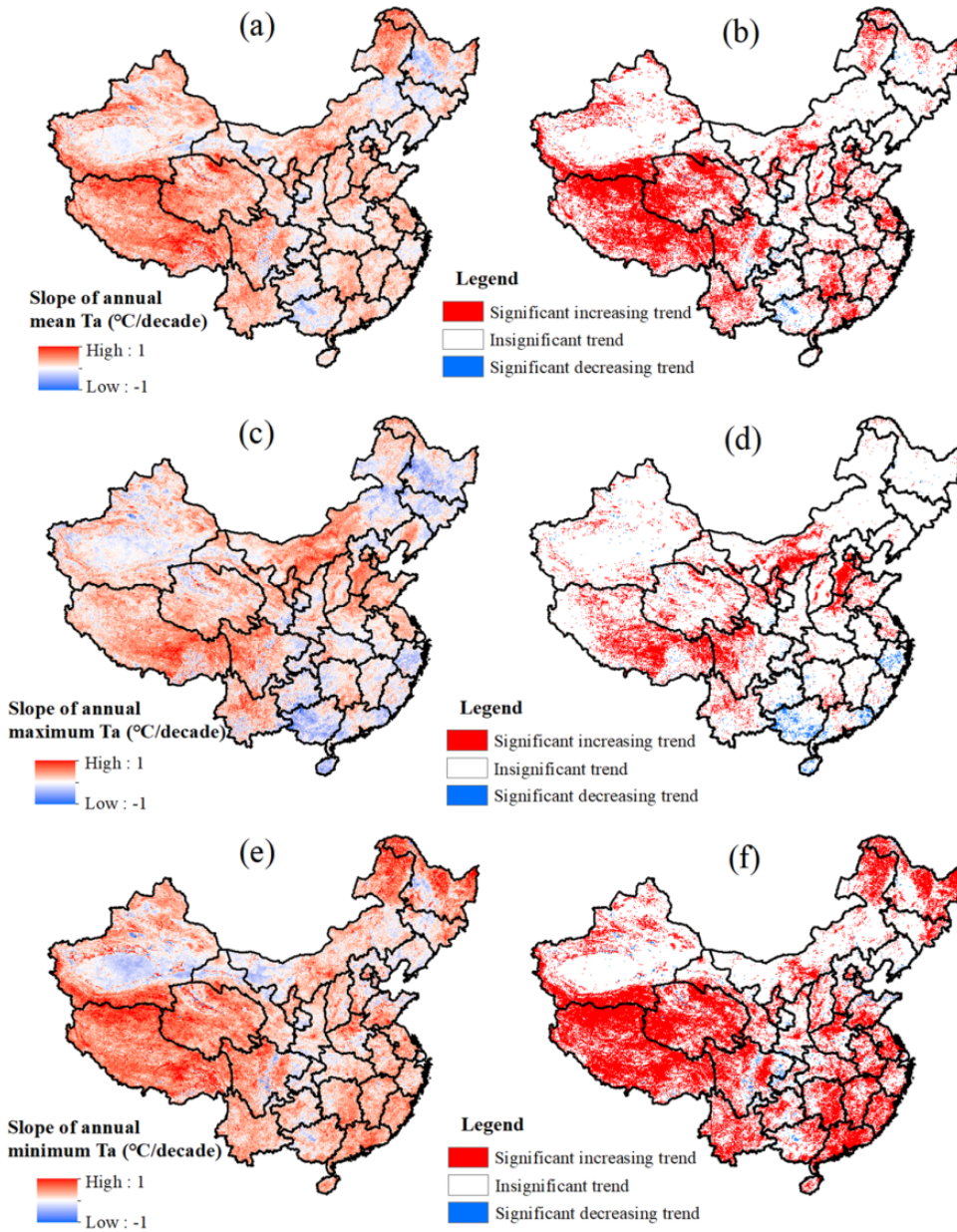


Figure 3. Temporal trends of Ta in mainland China: (a) trend of mean Ta; (b) significance of the trend of mean Ta; (c) trend of maximum Ta; (d) significance of the trend of maximum Ta; (e) trend of minimum Ta; (f) significance of the trend of minimum Ta.

of Ta were observed in spring (March to May) and summer (June to August) (Table 1). Spatially, the Tibetan Plateau generally showed higher increasing trends in Ta than other regions,

indicating that the Tibetan Plateau is sensitive to climate change. Additionally, significant decreasing trends were found in only a few areas in mainland China (Figure 3).

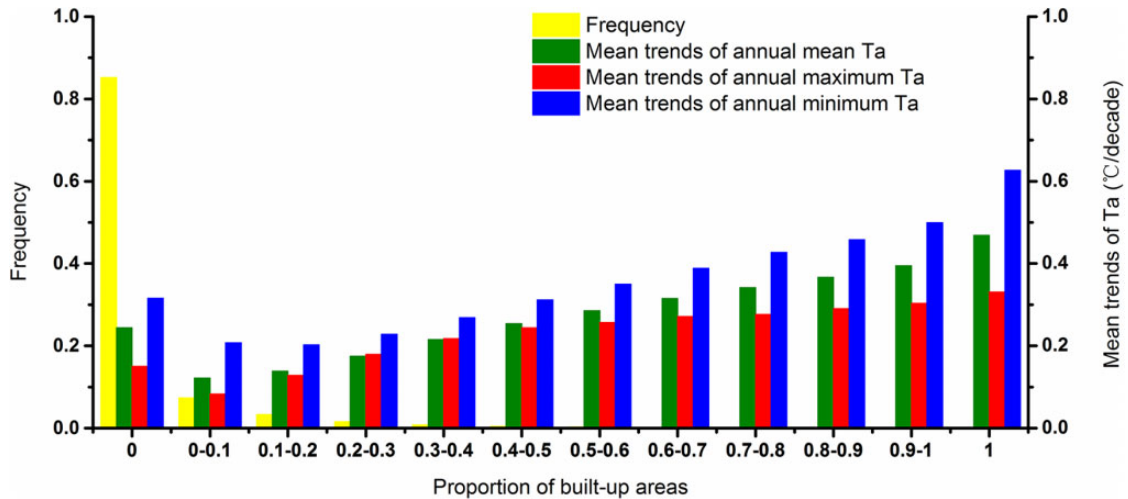


Figure 4. The frequency distribution of the proportion of built-up areas (yellow bar), and the mean trends of Ta of each range of proportions of built-up areas (green, red and blue bars).

3 Contribution of urbanization at the national scale

The annual mean Ta increased significantly at a rate of $0.23^{\circ}\text{C}/\text{decade}$ ($p < 0.1$) in mainland China. Once the effect of urbanization was excluded, the rate of increase was $0.23^{\circ}\text{C}/\text{decade}$ ($p < 0.1$) (Table 1). Thus, the effect of urbanization on the mean Ta was only $0.00^{\circ}\text{C}/\text{decade}$, and the contribution of urbanization was 0.98% at the national scale. In addition, the effects of urbanization on the trends of Ta at the national scale were also small for the annual maximum and minimum Ta, which was also the case for other seasons.

The small effects of urbanization on trends of Ta at the national scale can primarily be attributed to the low proportion of built-up areas in mainland China. The area of built-up areas was found to account for only 2.66% of the total area of mainland China in 2015 (derived from CLUD). Additionally, the frequency distribution of proportions of built-up areas and the mean trends of Ta of each range of proportions of built-up areas were calculated (using CLUD in 2015) (Figure 4). Three main results were

found. First, nonurbanized pixels account for 85.21% of mainland China (mainly in western China). This result suggested that the trends of Ta in most areas of China were not affected by urbanization. Second, the mean trends of the mean, maximum and minimum Ta in nonurbanized pixels were 0.24 , 0.15 and $0.32^{\circ}\text{C}/\text{decade}$, respectively. These values were close to the trends of the national average Ta (Table 1). This result suggested that even if there is no urbanization, the Ta will still rise significantly, another reason for the small contribution of urbanization to warming in mainland China in addition to the small proportion of built-up areas. Third, the trends of Ta generally increase with the increase in the proportion of built-up areas. The mean trend of minimum Ta in pixels with 100% built-up areas was even higher than $0.6^{\circ}\text{C}/\text{decade}$ (Figure 4). However, because urbanized pixels account for a small part of mainland China, the trends of the national average Ta were less affected by urbanized pixels.

The effects of urbanization on the trends of Ta and the contribution of urbanization to warming at the national scale in the present study were much lower than in some previous studies (Jin

et al., 2018; Ren and Ren, 2011; Ren and Zhou, 2014; Sun et al., 2016). A detailed discussion of this discrepancy is presented in section V.1.

4 Contribution of urbanization at the regional scale

The effects of urbanization on and the contribution of urbanization to warming trends were small in most areas in China (Figure 5). Spatially, the urbanization effect was higher than $0.02^{\circ}\text{C}/\text{decade}$, and the contribution of urbanization was higher than 10% in some areas in eastern China, especially on the North China Plain. In contrast, the effects of urbanization on the trends of Ta were small in western China. Additionally, there were some areas where there was an effect of urbanization on the trends in Ta of less than $0^{\circ}\text{C}/\text{decade}$, suggesting that Ta in rural areas increased more rapidly than in built-up areas. This increase can be explained by two main reasons. First, the proportion of built-up areas is close to zero in some regions. Thus, the urbanization effect was negligible and can be masked easily by local climate variability, land cover change in rural areas and random error. Second, changes in land cover in rural areas can alter the land surface properties and then alter the Ta.

Compared with mapping the contribution of urbanization to warming in each 250×250 km grid, the moving window method used in this study can provide more details of the contribution of urbanization to warming at the regional scale and can capture the extreme values (Figure 5). In addition, the effects of urbanization on the trends of Ta generally decrease as the window size increases, probably because the proportion of built-up areas in a window normally decreases as the window size increases.

5 Contribution of urbanization at the local scale

The contribution of urbanization to warming was substantial at the local scale (Figure 6 and

Table 2). The annual mean Ta in rural areas averaged for 31 cities increased insignificantly at a rate of $0.20^{\circ}\text{C}/\text{decade}$ ($p = 0.19$), which was lower than in the WUA ($0.42^{\circ}\text{C}/\text{decade}$, $p < 0.01$; Table 2). This result suggested that the effect of urbanization on the trend in mean Ta was $0.23^{\circ}\text{C}/\text{decade}$, and the contribution of urbanization to warming in the WUA was 53.18%. In addition, the effect of urbanization on the trends in minimum Ta ($0.26^{\circ}\text{C}/\text{decade}$) was larger than for the maximum Ta ($0.19^{\circ}\text{C}/\text{decade}$) in the WUA, similar to previous studies (Liao et al., 2017; Park et al., 2017; Ren and Zhou, 2014) and can be explained by the more pronounced UHI effect at night than in the daytime. Furthermore, the effects of urbanization on the trends in Ta in CUA were 0.24, 0.20 and $0.26^{\circ}\text{C}/\text{decade}$ for the mean, maximum and minimum Ta, respectively. These values were much higher than for SUA. These results are understandable since urbanization generally occurred in CUA rather than in SUA.

V Discussion

1 Overestimation of the contribution of urbanization at the national and regional scales in previous studies

Some previous studies showed that urbanization contributed substantially to warming in mainland China at the national scale (Jin et al., 2018; Ren and Ren, 2011; Ren and Zhou, 2014; Sun et al., 2016). For instance, Ren and Zhou (2014) found that the effect of urbanization on the trend of mean Ta was $0.05^{\circ}\text{C}/\text{decade}$, which contributed to 15.4% of the total warming during 1961–2008. Sun et al. (2016) showed that urbanization-induced warming was $0.09^{\circ}\text{C}/\text{decade}$, and the contribution of urbanization was approximately one-third for the period of 1961–2013. Jin et al. (2018) showed that the effect of urbanization on the trend in Ta was $0.05^{\circ}\text{C}/\text{decade}$, which accounted for 18% of the total warming during 1961–2012. Previous studies assessed the

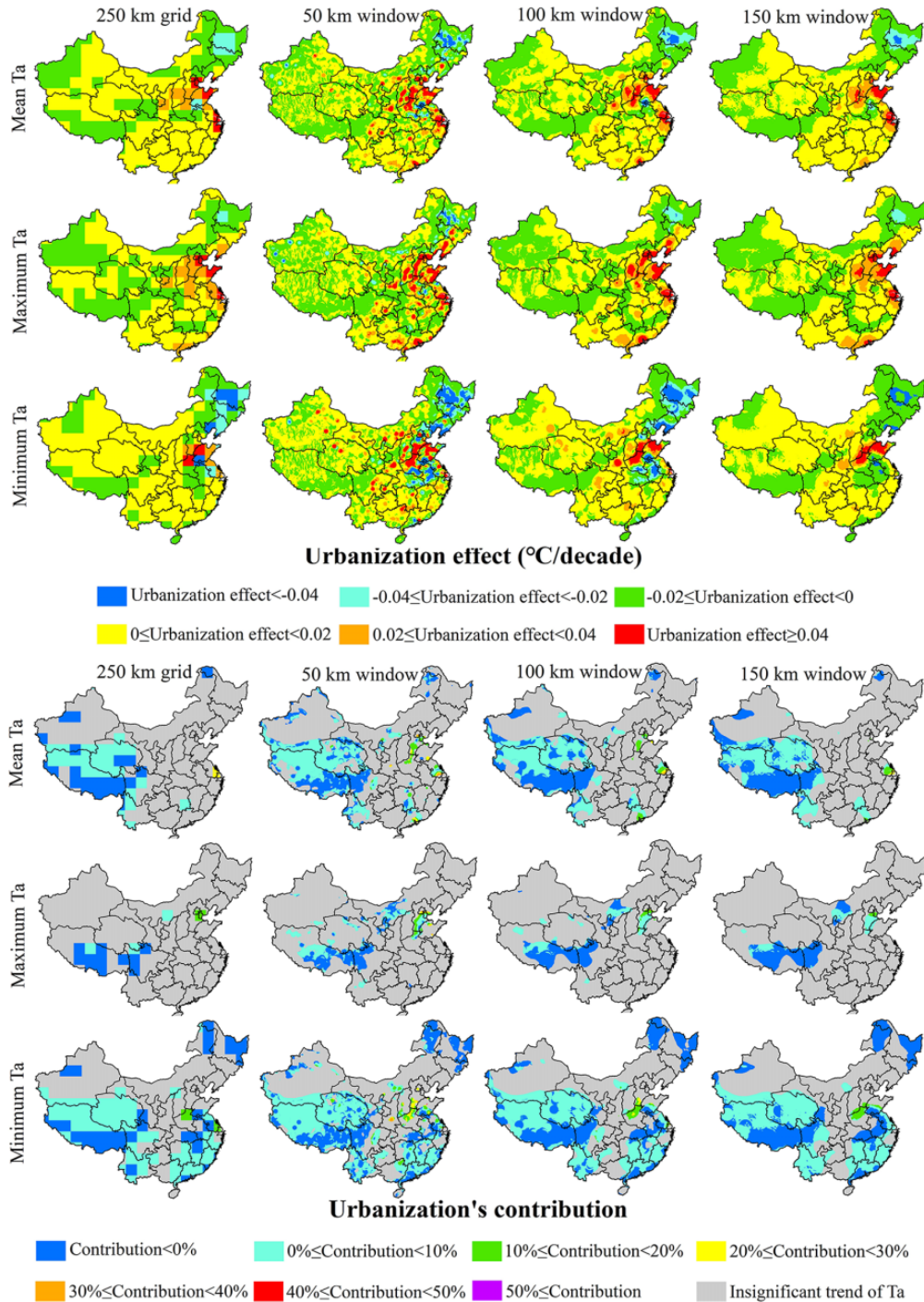


Figure 5. The effects of urbanization on and the contribution of urbanization to trends in Ta at the regional scale. There were no data in some areas because the trend of Ta was not statistically significant.

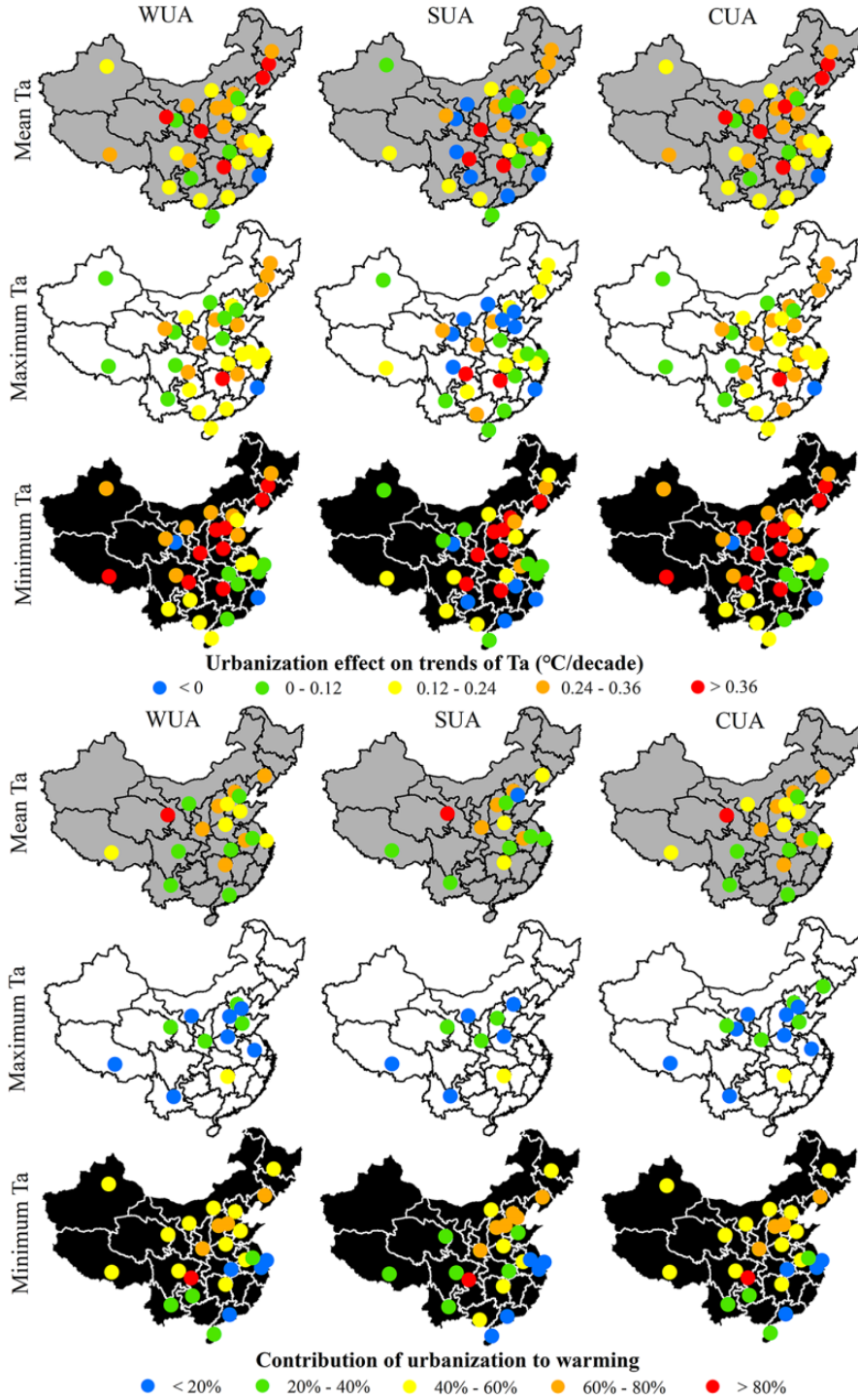


Figure 6. Effects of urbanization on and contribution of urbanization to trends in Ta at the local scale. Note that there were no data in some cities because the trend of Ta was not statistically significant.

Table 2. Trends in Ta averaged for 31 cities and the contribution of urbanization. The contribution of urbanization was only calculated when Ta in urban areas (WUA or SUA or CUA) increased significantly.

		WUA	SUA	CUA	Rural
Trends of Ta (°C/decade)	Annual mean Ta	0.42***	0.34**	0.44***	0.20
	Annual maximum Ta	0.35*	0.27	0.36*	0.16
	Annual minimum Ta	0.54***	0.50***	0.54***	0.28**
Urbanization's contribution	Annual mean Ta	53.18%	42.22%	54.29%	
	Annual maximum Ta	54.30%		55.87%	
	Annual minimum Ta	47.25%	42.52%	47.68%	

Significance levels: * $p < 0.1$; ** $p < 0.05$; *** $p < 0.01$.

contribution of urbanization to warming in mainland China using the following steps. First, mainland China was divided into a series of $5^\circ \times 5^\circ$ grids. Second, the trends in Ta and background Ta (without the effects of urbanization) in each grid were calculated as the average trend in Ta for all meteorological stations and rural meteorological stations, respectively. Third, the national average trends in Ta and background Ta were calculated as the area-weighted (weight was calculated according to the area of each grid) average trends in Ta and background Ta of all grids, respectively. Finally, the contribution of urbanization was calculated using equation (1) (Ren and Zhou, 2014; Sun et al., 2016). Similar methods were also utilized by many other studies in smaller study areas, and substantial contributions of urbanization to warming at the regional scale were found (Park et al., 2017; Qian et al., 2015; Ren et al., 2008; Wang and Yan, 2015; Yang et al., 2011; Zhou et al., 2004). However, a noteworthy issue is that simply arithmetically averaging trends in Ta from all meteorological stations within the grids may overestimate the total warming rate and the contribution of urbanization since most of the meteorological stations in mainland China are located in or around urban areas (Wang et al., 2015b). For example, in a $5^\circ \times 5^\circ$ grid composed of 20% urban area and 80% rural area, there are eight urban meteorological stations and two rural meteorological stations. If the trend in Ta of this grid were calculated as the arithmetically

averaged trend of Ta from all meteorological stations, the total warming rate and the contribution of urbanization may be overestimated since the proportion of urban meteorological stations to total meteorological stations (80%) is much higher than the proportion of urban area to total area (20%). In addition, we can infer that if the number of rural meteorological stations increases, the trend in Ta of a grid calculated using this method will decrease. Wang et al. (2015a) first proposed this viewpoint and used an area-weighted (percentages of urban and rural areas in a grid were utilized as the weights) average method to generate the trends in Ta for grids. Their results showed that the contribution of urbanization to warming in mainland China was approximately 0.35% (during 1951–2010), which was relatively close to the present study. However, the view of Wang et al. (2015a) is accepted and supported by few studies. Additionally, the view of Wang et al. (2015b) is based on the hypothesis that the Ta from nominal urban (or rural) meteorological stations can represent the Ta of the entirety of urban (or rural) areas, which may lead to some uncertainties.

Some studies found that the contribution of urbanization to warming at the national scale was negligible (Li et al., 2004, 2019; Shao et al., 2011; Wang et al., 2015b). Among these studies, Li et al. (2004) first gave the right result. As their methods were used by few studies, they are not discussed in detail in this paper.

2 Underestimation of the contribution of urbanization at the local scale in previous studies

Previous studies found that the contributions of urbanization to the observed warming trends at the local scale were generally between 10 and 40% (Liao et al., 2017; Ren et al., 2008; Wang and Ge, 2012; Wang et al., 2015a; Yang et al., 2011; Zhao et al., 2014), which were lower than for this study. Most meteorological stations are located in or around urban areas in China, and reliable reference rural stations are scarce. As a result, previous studies may underestimate the contribution of urbanization at the local scale. This underestimation was acknowledged by previous studies (Liao et al., 2017; Ren and Zhou, 2014; Ren et al., 2008; Yang et al., 2011). Furthermore, the trends in T_a in SUA were different from the trends in CUA, similar to previous studies (Yao et al., 2017; Zhao and Wu, 2017). These findings highlight the importance of using spatially continuous data to assess the contribution of urbanization to warming. Previous studies usually used one meteorological station to represent the T_a of an entire city, which may cause some uncertainties.

3 The reliability of the results

In the present study, a series of methods to evaluate the contribution of urbanization to warming were proposed. When analyzing the contribution of urbanization to warming at the national scale, urbanized pixels were replaced as the average T_a of nonurbanized pixels within a radius of 50 km. At the local scale, nonurbanized pixels in 50 km buffers around the cities were defined as reference rural areas. The 50 km threshold mentioned above is slightly arbitrary. Therefore, we further tested the sensitivity and robustness of the results of the effects of urbanization on trends in T_a to different thresholds. Thresholds of 30 and 70 km were also used. The results showed that different thresholds did not yield significant differences in the effects

Table 3. The sensitivity and robustness of the results of the effects of urbanization on the trends in T_a at the national scale ($^{\circ}\text{C}/\text{decade}$) for different thresholds. All data were rounded up to two decimal places. The minus sign indicates that the effect of urbanization on the trends in T_a is negative.

	Mean T_a	Maximum T_a	Minimum T_a
30 km was selected as threshold	0.00	-0.00	0.00
50 km was selected as threshold	0.00	-0.00	0.00
70 km was selected as threshold	0.00	0.00	-0.00

of urbanization on the trends in T_a at the national scale (Table 3). The effects of urbanization on the trends in T_a were lower than $0.00^{\circ}\text{C}/\text{decade}$ in all cases. At the local scale, effects of urbanization on the trends in T_a increased with the increase in the threshold (Table 4). Further analyses showed that this increase can be explained by different climate regimes. For instance, T_a decreased significantly in some areas in 50–70 km buffers around Xi'an and Chengdu. Therefore, if a 70 km buffer was set as the threshold, the effects of urbanization on the trends in T_a would increase. To reduce the effect of different climate regimes, rural areas were not selected as areas beyond 50 km in the present study.

4 The advantages of satellite-based methods

Satellite-based methods developed in this study have a number of advantages compared to station-based methods in previous studies. First, when assessing the contribution of urbanization at the national and regional scales, previous studies calculated the T_a of a grid as the average T_a of all meteorological stations in that grid. This calculation may lead to certain uncertainties according to the previous section. Comparatively, satellite remote sensing can provide wall-to-wall observational coverage, and the T_a of a region can be computed simply as the average T_a of all pixels.

Table 4. The sensitivity and robustness of the results of the effect of urbanization on the trends in Ta at the local scale in the WUA ($^{\circ}\text{C}/\text{decade}$) for different thresholds.

	Mean Ta	Maximum Ta	Minimum Ta
30 km was selected as threshold	0.20	0.17	0.22
50 km was selected as threshold	0.23	0.19	0.26
70 km was selected as threshold	0.24	0.21	0.27

Second, when assessing the contribution of urbanization at the regional scale, previous studies can only investigate the contribution of urbanization to warming in each $2.5^{\circ} \times 2.5^{\circ}$ or $5^{\circ} \times 5^{\circ}$ grid. In the present study, the contribution of urbanization can be revealed more thoroughly using a moving window method (Figure 5). Third, previous studies used nominal urban and rural meteorological stations to assess the contribution of urbanization, which may lead to some uncertainties. For example, the rural stations utilized in previous studies were not purely rural stations, and the Ta of a city was usually represented by only one station. In this study, these uncertainties can be avoided by the use of spatially continuous satellite observations, and the contribution of urbanization can be more accurately evaluated.

5 Limitations

Satellite-based methods have some limitations. First, MODIS Ts data are available from February 2000 to the present. Therefore, the study period in this study is only 18 years, which is relatively short to reveal climate change. The warming trends and the contribution of urbanization to warming in this study will be affected by internal climate variability and atmospheric oscillations. Future studies should use longer time series data to analyze the contribution of urbanization to warming. Second, the accuracy of the estimated Ta is evidently lower than the

accuracy of the in situ Ta. This may lead to some uncertainties. However, we believe that with the increasing accuracy of the estimated Ta (e.g. with the improvements in Ts data and the estimation method), these uncertainties will decrease.

VI Conclusions

In this study, the contribution of urbanization to warming during 2001–2018 was systematically estimated at the national, regional and local scales using satellite estimated Ta data. A Cubist model produced satisfactory Ta estimation accuracy with RMSEs between 1.15 and 1.51°C . The national average Ta was found to increase significantly ($0.23^{\circ}\text{C}/\text{decade}$, $p < 0.1$). At the national scale, the contribution of urbanization to warming was less than 1%, primarily because built-up areas account for only 2.66% of China's area. At the regional scale, the contribution of urbanization was also small in most cases and was even negative in some areas. The contribution of urbanization was overestimated at the national and regional scales by many previous studies, because previous studies used the simple average method to calculate regional average Ta. At the local scale, the contributions of urbanization to warming were 53.18%, 54.30% and 47.25% for the mean, maximum and minimum Ta, respectively, averaged for 31 major cities. The contribution of urbanization was underestimated at the local scale by previous studies, because they used nominal rural stations to calculate the contribution of urbanization.

Satellite-based methods developed in this study have a number of advantages compared to station-based methods in previous studies. First, the proposed method in this study can avoid uncertainties when calculating the contributions of urbanization. Second, the moving window method can reveal the contribution of urbanization at the regional scale more thoroughly. However, limitations also exist in the

present study. First, the study period in the present study is relatively short because MODIS data have been available only since February 2000. Second, the accuracy of the estimated Ta is lower than that of the in situ Ta. Future studies should: (1) use longer time series data to analyze the contribution of urbanization to warming; and (2) simultaneously use the Ta monitored by meteorological stations and the Ta estimated by remote sensing to study the effects of urbanization.


Declaration of conflicting interests

The authors have no conflicts of interest to declare.

Funding

The authors disclosed receipt of the following financial support for the research, authorship, and/or publication of this article: This work was supported by the National Natural Science Foundation of China (grant numbers 41601044 and 41975044), the Special Fund for Basic Scientific Research of Central Colleges, China University of Geosciences, Wuhan (CUGCJ1704) and the Fundamental Research Funds for National Universities, China University of Geosciences (Wuhan).

ORCID iD

Lunche Wang  <https://orcid.org/0000-0001-7783-5725>

References

- Benali A, Carvalho AC, Nunes JP, et al. (2012) Estimating air surface temperature in Portugal using MODIS LST data. *Remote Sensing of Environment* 124: 108–121.
- Chen Y, Quan J, Zhan W, et al. (2016) Enhanced statistical estimation of air temperature incorporating nighttime light data. *Remote Sensing* 8: 656.
- Fall S, Niyogi D, Gluhovsky A, et al. (2010) Impacts of land use land cover on temperature trends over the continental United States: Assessment using the North American Regional Reanalysis. *International Journal of Climatology* 30: 1980–1993.
- Fang F, Guo J, Sun L, et al. (2014) The effects of urbanization on temperature trends in different economic periods and geographical environments in northwestern China. *Theoretical and Applied Climatology* 116: 227–241.
- Good EJ, Ghent DJ, Bulgin CE, et al. (2017) A spatio-temporal analysis of the relationship between near-surface air temperature and satellite land surface temperatures using 17 years of data from the ATSR series. *Journal of Geophysical Research: Atmospheres* 122: 9185–9210.
- Hansen J, Ruedy R, Sato M, et al. (2010) Global surface temperature change. *Reviews of Geophysics* 48: RG4004.
- Hooker J, Duveiller G and Cescatti A (2018) A global dataset of air temperature derived from satellite remote sensing and weather stations. *Scientific Data* 5: 180246.
- Huete A, Didan K, Miura T, et al. (2002) Overview of the radiometric and biophysical performance of the MODIS vegetation indices. *Remote Sensing of Environment* 83: 195–213.
- Imhoff ML, Zhang P, Wolfe RE, et al. (2010) Remote sensing of the urban heat island effect across biomes in the continental USA. *Remote Sensing of Environment* 114: 504–513.
- Jin K, Wang F, Yu Q, et al. (2018) Varied degrees of urbanization effects on observed surface air temperature trends in China. *Climate Research* 76: 131–143.
- Kalnay E and Cai M (2003) Impact of urbanization and land-use change on climate. *Nature* 423: 528–531.
- Kalnay E, Cai M, Li H, et al. (2006) Estimation of the impact of land-surface forcings on temperature trends in eastern United States. *Journal of Geophysical Research* 111: D06106.
- Karl TR, Diaz HF and Kukla G (1988) Urbanization: Its detection and effect in the united states climate record. *Journal of Climate* 1: 1099–1123.
- Kuang W, Liu J, Dong J, et al. (2016) The rapid and massive urban and industrial land expansions in China between 1990 and 2010: A CLUD-based analysis of their trajectories, patterns, and drivers. *Landscape and Urban Planning* 145: 21–33.
- Li L and Zha Y (2019) Estimating monthly average temperature by remote sensing in China. *Advances in Space Research* 63: 2345–2357.
- Li Q, Zhang H, Liu X, et al. (2004) Urban heat island effect on annual mean temperature during the last 50 years in China. *Theoretical and Applied Climatology* 79: 165–174.
- Li X, Zhou Y, Asrar GR, et al. (2018) Developing a 1 km resolution daily air temperature dataset for urban and

- surrounding areas in the conterminous United States. *Remote Sensing of Environment* 215: 74–84.
- Li Y, Wang L, Zhou H, et al. (2019) Urbanization effects on changes in the observed air temperatures during 1977–2014 in China. *International Journal of Climatology* 39: 251–265.
- Liao W, Wang D, Liu X, et al. (2017) Estimated influence of urbanization on surface warming in Eastern China using time-varying land use data. *International Journal of Climatology* 37: 3197–3208.
- Lin X, Zhang W, Huang Y, et al. (2016) Empirical estimation of near-surface air temperature in China from MODIS LST data by considering physiographic features. *Remote Sensing* 8: 629.
- Liu J, Kuang W, Zhang Z, et al. (2014) Spatiotemporal characteristics, patterns, and causes of land-use changes in China since the late 1980s. *Journal of Geographical Sciences* 24: 195–210.
- Lu N, Liang S, Huang G, et al. (2018) Hierarchical Bayesian space-time estimation of monthly maximum and minimum surface air temperature. *Remote Sensing of Environment* 211: 48–58.
- Luo M and Lau NC (2017) Heat waves in southern China: Synoptic behavior, long-term change, and urbanization effects. *Journal of Climate* 30: 703–720.
- Mertes CM, Schneider A, Sulla-Menashe D, et al. (2015) Detecting change in urban areas at continental scales with MODIS data. *Remote Sensing of Environment* 158: 331–347.
- Mohsin T and Gough WA (2010) Trend analysis of long-term temperature time series in the Greater Toronto Area (GTA). *Theoretical and Applied Climatology* 101: 311–327.
- Niu Z, Wang L, Niu Y, et al. (2018) Spatiotemporal variations of photosynthetically active radiation and the influencing factors in China from 1961 to 2016. *Theoretical and Applied Climatology* 137: 2049–2067.
- Noi P, Degener J and Kappas M (2017) Comparison of multiple linear regression, Cubist regression, and random forest algorithms to estimate daily air surface temperature from dynamic combinations of MODIS LST data. *Remote Sensing* 9: 398.
- Park BJ, Kim YH, Min SK, et al. (2017) Long-term warming trends in Korea and contribution of urbanization: An updated assessment. *Journal of Geophysical Research-Atmospheres* 122: 10637–10654.
- Parker DE (2006) A demonstration that large-scale warming is not urban. *Journal of Climate* 19: 2882–2895.
- Právělie R (2018) Major perturbations in the Earth's forest ecosystems. Possible implications for global warming. *Earth-Science Reviews* 185: 544–571.
- Qian C, Ren G and Zhou Y (2015) Urbanization effects on climatic changes in 24 particular timings of the seasonal cycle in the middle and lower reaches of the Yellow River. *Theoretical and Applied Climatology* 124: 781–791.
- Quinlan JR (1992) Learning with Continuous Classes. *Proceedings of Australian Joint Conference on Artificial Intelligence*, Hobart, Tasmania, 16–18 November 1992, pp. 343–348.
- Ren G and Zhou Y (2014) Urbanization effect on trends of extreme temperature indices of national stations over mainland China, 1961–2008. *Journal of Climate* 27: 2340–2360.
- Ren G, Ding Y and Tang G (2017) An overview of mainland China temperature change research. *Journal of Meteorological Research* 31: 3–16.
- Ren G, Zhou Y, Chu Z, et al. (2008) Urbanization effects on observed surface air temperature trends in north China. *Journal of Climate* 21: 1333–1348.
- Ren Y and Ren G (2011) A remote-sensing method of selecting reference stations for evaluating urbanization effect on surface air temperature trends. *Journal of Climate* 24: 3179–3189.
- Roe GH, Baker MB and Herla F (2016) Centennial glacier retreat as categorical evidence of regional climate change. *Nature Geoscience* 10: 95–99.
- Shakhova N, Semiletov I, Gustafsson O, et al. (2017) Current rates and mechanisms of subsea permafrost degradation in the East Siberian Arctic Shelf. *Nature Communications* 8: 15872.
- Shao Q, Sun C, Liu J, et al. (2011) Impact of urban expansion on meteorological observation data and overestimation to regional air temperature in China. *Journal of Geographical Sciences* 21: 994–1006.
- Shi L, Liu P, Kloog I, et al. (2016) Estimating daily air temperature across the Southeastern United States using high-resolution satellite data: A statistical modeling study. *Environmental Research* 146: 51–58.
- Shi Z, Jia G, Hu Y, et al. (2019) The contribution of intensified urbanization effects on surface warming trends in China. *Theoretical and Applied Climatology* 138: 1125–1137.
- Shiflett SA, Liang LL, Crum SM, et al. (2017) Variation in the urban vegetation, surface temperature, air temperature nexus. *Science of the Total Environment* 579: 495–505.

- Sun Y, Zhang X, Ren G, et al. (2016) Contribution of urbanization to warming in China. *Nature Climate Change* 6: 706–709.
- Sun Y, Zhang X, Zwiers FW, et al. (2014) Rapid increase in the risk of extreme summer heat in Eastern China. *Nature Climate Change* 4: 1082–1085.
- Tachikawa T, Kaku M, Iwasaki A, et al. (2011) ASTER Global Digital Elevation Model version 2 – summary of validation results. Available at: http://www.jspacesystems.or.jp/ersdac/GDEM/ver2Validation/Summary_GDEM2_validation_report_final.pdf (accessed 24 January 2020).
- United Nations (2018) *World Urbanization Prospects: The 2018 Revision*. Department of Economic and Social Affairs, New York, United Nations.
- Wang F and Ge Q (2012) Estimation of urbanization bias in observed surface temperature change in China from 1980 to 2009 using satellite land-use data. *Chinese Science Bulletin* 57: 1708–1715.
- Wang F, Ge Q, Wang S, et al. (2015a) A new estimation of urbanization's contribution to the warming trend in China. *Journal of Climate* 28: 8923–8938.
- Wang J, Huang B, Fu D, et al. (2015b) Spatiotemporal variation in surface urban heat island intensity and associated determinants across major Chinese cities. *Remote Sensing* 7: 3670–3689.
- Wang L, Liu B, Henderson M, et al. (2018) Warming across decades and deciles: Minimum and maximum daily temperatures in China, 1955–2014. *International Journal of Climatology* 38: 2325–2332.
- Wang M and Yan X (2015) A comparison of two methods on the climatic effects of urbanization in the Beijing-Tianjin-Hebei metropolitan area. *Advances in Meteorology* 2015: 352360.
- Weng Q (2009) Thermal infrared remote sensing for urban climate and environmental studies: Methods, applications, and trends. *ISPRS Journal of Photogrammetry and Remote Sensing* 64: 335–344.
- Xu Y, Knudby A, Shen Y, et al. (2018) Mapping monthly air temperature in the Tibetan Plateau from MODIS data based on machine learning methods. *IEEE Journal of Selected Topics in Applied Earth Observations and Remote Sensing* 11: 345–354.
- Yang X, Hou Y and Chen B (2011) Observed surface warming induced by urbanization in east China. *Journal of Geophysical Research* 116: D14113.
- Yao R, Wang L, Huang X, et al. (2017) Temporal trends of surface urban heat islands and associated determinants in major Chinese cities. *Science of the Total Environment* 609: 742–754.
- Yao R, Wang L, Huang X, et al. (2018) The influence of different data and method on estimating the surface urban heat island intensity. *Ecological Indicators* 89: 45–55.
- Yao R, Wang L, Huang X, et al. (2019) Greening in rural areas increases the surface urban heat island intensity. *Geophysical Research Letters* 46: 2204–2212.
- Yoo C, Im J, Park S, et al. (2018) Estimation of daily maximum and minimum air temperatures in urban landscapes using MODIS time series satellite data. *ISPRS Journal of Photogrammetry and Remote Sensing* 137: 149–162.
- Zhang H, Zhang F, Ye M, et al. (2016) Estimating daily air temperatures over the Tibetan Plateau by dynamically integrating MODIS LST data. *Journal of Geophysical Research-Atmospheres* 121: 11425–11441.
- Zhao D and Wu J (2017) The influence of urban surface expansion in China on regional climate. *Journal of Climate* 30: 1061–1080.
- Zhao P, Jones P, Cao L, et al. (2014) Trend of surface air temperature in eastern China and associated large-scale climate variability over the last 100 years. *Journal of Climate* 27: 4693–4703.
- Zhou D, Zhao S, Liu S, et al. (2014) Surface urban heat island in China's 32 major cities: Spatial patterns and drivers. *Remote Sensing of Environment* 152: 51–61.
- Zhou D, Zhao S, Zhang L, et al. (2015) The footprint of urban heat island effect in China. *Scientific Reports* 5: 11160.
- Zhou L, Dickinson RE, Tian Y, et al. (2004) Evidence for a significant urbanization effect on climate in China. *Proceedings of the National Academy of Sciences of the United States of America* 101: 9540–9544.
- Zhu W, Lú A and Jia S (2013) Estimation of daily maximum and minimum air temperature using MODIS land surface temperature products. *Remote Sensing of Environment* 130: 62–73.
- Zhu X, Zhang Q, Xu CY, et al. (2019) Reconstruction of high spatial resolution surface air temperature data across China: A new geo-intelligent multisource data-based machine learning technique. *Science of the Total Environment* 665: 300–313.